

Synthesis of Linear, Cyclic, Figure-Eight-Shaped, and Tadpole-Shaped Amphiphilic Block Copolyethers via *t*-Bu-P₄-Catalyzed Ring-Opening Polymerization of Hydrophilic and Hydrophobic Glycidyl Ethers

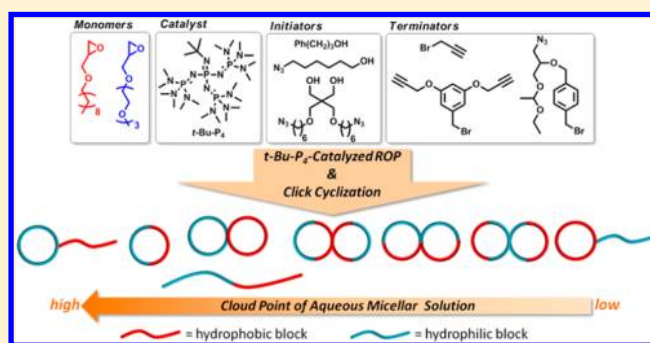
Takuya Isono,[†] Yusuke Satoh,[†] Kana Miyachi,[†] Yougen Chen,[‡] Shin-ichiro Sato,[‡] Kenji Tajima,[‡] Toshifumi Satoh,^{*,‡} and Toyoji Kakuchi^{*,‡}

[†]Graduate School of Chemical Sciences and Engineering, Hokkaido University, Sapporo 060-8628, Japan

[‡]Division of Biotechnology and Macromolecular Chemistry, Faculty of Engineering, Hokkaido University, Sapporo 060-8628, Japan

S Supporting Information

ABSTRACT: This paper describes the synthesis of systematic sets of figure-eight- and tadpole-shaped amphiphilic block copolyethers (BCPs) consisting of poly(decyl glycidyl ether) and poly[2-(2-(2-methoxyethoxy)ethoxy)ethyl glycidyl ether], together with the corresponding cyclic counterparts, via combination of the *t*-Bu-P₄-catalyzed ring-opening polymerization (ROP) and click cyclization. The clickable linear BCP precursors, with precisely controlled azido and ethynyl group placements as well as a fixed molecular weight and monomer composition (degree of polymerization for each block was adjusted to be around 50), were prepared by the *t*-Bu-P₄-catalyzed ROP with the aid of functional initiators and terminators. The click cyclization of the precursors under highly diluted conditions produced a series of cyclic, figure-eight-, and tadpole-shaped BCPs with narrow molecular weight distributions of less than 1.06. Preliminary studies of the BCPs self-assembly in water revealed the significant variation in their cloud points depending on the BCP architecture, though there were small architectural effects on their critical micelle concentration and morphology of the aggregates.



INTRODUCTION

Macromolecules possessing cyclic architectures, such as cyclic, figure-eight-shaped, and tadpole-shaped polymers, are of great interest due to the endless nature of the cyclic chain, which endowed them with an increased glass transition temperature, lower viscosity, and smaller hydrodynamic volume.^{1–6} In addition, the cyclic block copolymers (BCPs) provided special properties in relation to self-assembly, which are typically not attainable with the corresponding linear counterparts.^{7–15} For example, Tezuka and Yamamoto et al. reported an increase in the thermal stability of micelles formed from cyclic poly(ethylene oxide)-*block*-poly(butyl acrylate) as compared to the corresponding linear counterpart.^{7–9} Recently, Hawker et al. demonstrated the control of a microphase-separated structure in cylinder-forming poly(ethylene oxide)-*block*-poly(styrene) via macrocyclization, which enabled a ca. 30% decrease in the domain spacing.¹² Although many synthetic approaches for cyclic BCPs have been established,^{3–5} the synthesis of cyclic-containing BCPs, such as figure-eight- and tadpole-shaped BCPs, is still a remaining and challenging task. A comprehensive sets of such BCPs, i.e., linear, cyclic, figure-eight-shaped, and tadpole-shaped BCPs, possessing comparable chemical structures, monomer compositions, and molecular

weights have been never achieved, though there were several reports about synthesizing tadpole- and figure-eight-shaped BCPs, such as [cyclic poly(chloroethyl vinyl ether)]-*block*-polystyrene,¹⁶ (cyclic-polystyrene)-*block*-poly(ethylene oxide),¹⁷ [cyclic-poly(ethylene oxide)]-*block*-polystyrene,¹⁸ [cyclic-poly(*N*-isopropylacrylamide)]-*block*-poly(ϵ -caprolactone),¹⁹ (cyclic-polystyrene)-*block*-[cyclic-poly(ϵ -caprolactone)],²⁰ [cyclic-poly(ethylene oxide)]-*block*-[cyclic-poly(tetrahydrofuran)],²¹ cyclic-[poly(ethylene oxide)-*block*-polystyrene],²² and (cyclic-polystyrene)-*block*-poly(acrylic acid).²³ To provide a fundamental insight into the relationship between the cyclic-containing topology and self-assembling property, a concise and robust strategy is required for preparing figure-eight- and tadpole-shaped BCPs possessing varied block arrangements.

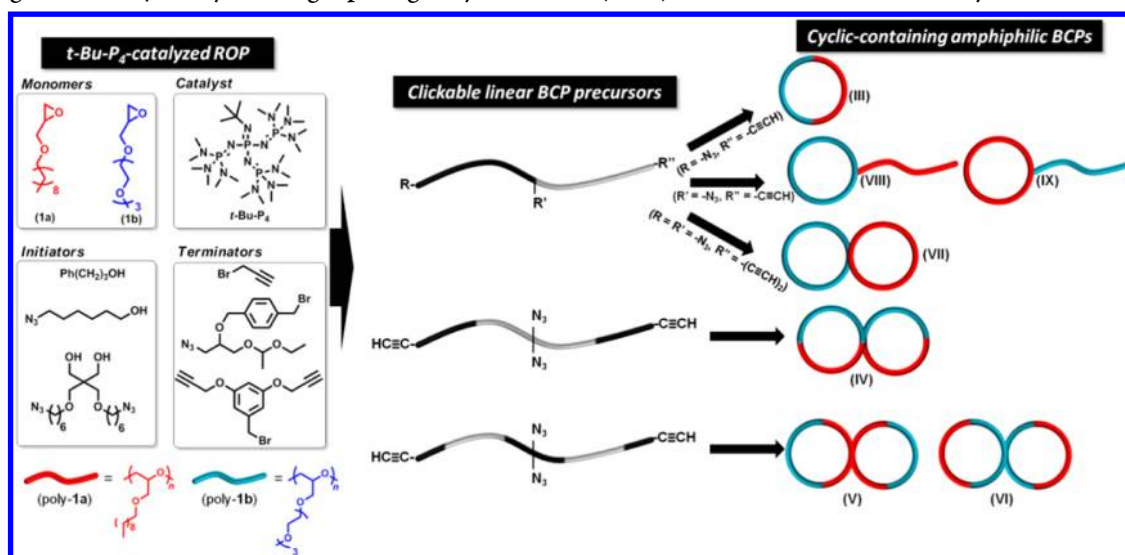
Among the wide range of BCP systems, polyether-based amphiphilic BCPs, which are obtained via the ring-opening polymerization (ROP) of epoxy monomers, have been recognized as the most traditional but important class of

Received: March 7, 2014

Revised: April 8, 2014

Published: April 16, 2014

Scheme 1. Synthesis of Cyclic, Figure-Eight-Shaped, and Tadpole-Shaped Amphiphilic Block Copolyethers (BCPs) by Combining the *t*-Bu-P₄-Catalyzed Ring-Opening Polymerization (ROP) and Intramolecular Click Cyclization



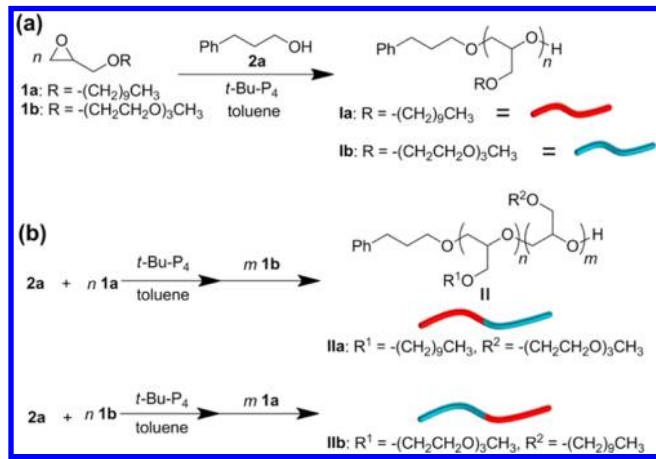
BCP materials due to their nonionic character, good chemical stability, biocompatibility, and low toxicity, and such BCPs were commercialized for applications as a nonionic surfactant, functional fluid, emulsifier, and carrier for drug delivery.^{24–26} Indeed, there has been considerable efforts to investigate the self-assembly of polyether-based BCPs, such as the poly(ethylene oxide) (PEO)/poly(propylene oxide) (PPO), PEO/poly(butylene oxide) (PBO), and poly(glycidol)/PPO BCP systems, in both the bulk and solution states during the past several decades.^{25,27–30} These elaborated studies have revealed that the block arrangement, e.g., AB type diblock or ABA and BAB type triblocks,^{31,32} as well as macromolecular architectures, e.g., linear and macrocyclic structures,^{33,34} affect the BCP self-assembling properties, such as micelle size, morphology, critical micelle concentration, critical micelle temperature, and cloud point in aqueous solution. However, there is less information available about the topological effects on the self-assembly. The synthesis of polyether-based BCPs possessing a macrocyclic architecture was achieved by the acetalization of PEO-*b*-PPO-*b*-PEO or PEO-*b*-PBO-*b*-PEO triblock copolymers through the reaction of a hydroxyl end group with dichloromethane under Williamson conditions and high dilution.^{33,34} However, this methodology is hard to use for the synthesis of polyether-based BCPs with figure-eight- and tadpole-shaped architectures. The intramolecular click reactions of α -azido, ω -ethynyl- (or α -ethynyl, ω -azido-) functionalized precursors have emerged as a powerful mean for constructing cyclic polymers and cyclic BCPs.^{35,36} Such a highly efficient method should be expandable for the synthesis of polyether-based BCPs with figure-eight- and tadpole-shaped architectures by combining the appropriately designed precursor BCPs with precisely controlled azido and ethynyl group placements as well as a fixed molecular weight and monomer composition. Toward this contribution, we recently demonstrated that 1-*tert*-butyl-4,4,4-tris(dimethylamino)-2,2-bis[tris(dimethylamino)phosphoranylideneamino]-2,2,5,4,4,5-catenadi(phosphazene) (*t*-Bu-P₄)-catalyzed ROP was an effective method to synthesize well-defined polyethers with various end-functionalities from a wide range of substituted epoxy monomers, which was further applied for the precise synthesis of linear diblock copolyethers.^{37–39} In addition, a combination of the *t*-Bu-P₄-

catalyzed ROP and intramolecular click cyclization was found to be an efficient route for the synthesis of cyclic and figure-eight-shaped polyethers.⁴⁰ We now describe a novel approach to provide systematic sets of figure-eight- and tadpole-shaped amphiphilic BCPs via the intramolecular click reaction of linear BCP precursors bearing azido and ethynyl functionalities at designed positions, together with the corresponding linear and cyclic counterparts, as shown in Scheme 1. The clickable linear BCP precursors were precisely synthesized based on the *t*-Bu-P₄-catalyzed ROP of decyl glycidyl ether (**1a**) as a hydrophobic monomer and 2-(2-(2-methoxyethoxy)ethoxy)ethyl glycidyl ether (**1b**) as a hydrophilic monomer with the combination of functional initiators and terminators. We initially examined the homopolymerization and block copolymerization of **1a** and **1b** to ensure the well-controlled nature of the *t*-Bu-P₄-catalyzed ROP system. The intramolecular click reaction of α -azido, ω -ethynyl-functionalized poly-**1a**-*block*-poly-**1b** was then examined to produce the cyclic BCP and to provide fundamental insight into the cyclization conditions. Finally, the combination of the *t*-Bu-P₄-catalyzed ROP and intramolecular click cyclization was applied to clickable linear precursors with various di-, tri-, and pentablock sequences for producing figure-eight-shaped BCPs with four different block arrangements and tadpole-shaped BCPs with two different block arrangements. A preliminary study of the self-assembling properties in water was performed using the obtained linear, cyclic, figure-eight-shaped, and tadpole-shaped BCPs.

RESULTS AND DISCUSSION

To confirm the polymerization properties of decyl glycidyl ether (**1a**) and 2-(2-(2-methoxyethoxy)ethoxy)ethyl glycidyl ether (**1b**), the *t*-Bu-P₄-catalyzed ROPs of **1a** and **1b** were conducted before the synthesis of the block copolymers. The polymerizations of **1a** and **1b** were carried out using 3-phenyl-1-propanol (**2a**) as the initiator at the [monomer]₀/[**2a**]₀/[*t*-Bu-P₄]₀ ratio of 25/1/1 in toluene at room temperature (Scheme 2a). The monomer conversions of **1a** and **1b** reached >99% within 20 h to produce the narrowly dispersed poly-**1a** (**1a**) and poly-**1b** (**1b**) with the number-average molecular weights determined from the NMR ($M_{n,NMR}$) of 5710 and 5750 g mol⁻¹, respectively. The M_n s ($M_{n,clcd}$) calculated from

Scheme 2. (a) Homopolymerization and (b) Block Copolymerization for Decyl Glycidyl Ether (**1a**) and 2-(2-(2-Methoxyethoxy)ethoxy)ethyl Glycidyl Ether (**1b**)



the initial monomer-to-initiator ratio and monomer conversion matched the $M_{n,NMR}$ s of **1a** and **1b**, indicating the controlled nature of the $t\text{-Bu-P}_4$ -catalyzed ROP systems. The NMR and matrix-assisted laser desorption/ionization mass spectral analyses of the obtained polymers revealed that the polymerizations of **1a** and **1b** proceeded without side reactions, such as the transfer reaction to the monomer⁴¹ (Table S1, Figures S1–S3). Based on the results, the linear amphiphilic diblock copolymers, **IIa** and **IIb**, were then synthesized via the sequential block copolymerization of **1a** and **1b**, as shown in Scheme 2b. Unless otherwise noted, the number-average degree of polymerization (DP) of the targeted BCP (poly-**1a**/poly-**1b**) is adjusted to be around 100 (50/50). A poly-**1a** with the $M_{n,NMR}$ of 10 800 g mol⁻¹ and M_w/M_n of 1.03 was first prepared by the $t\text{-Bu-P}_4$ -catalyzed ROP of **1a** using **2a** as the initiator with the perfect monomer conversion at the $[\mathbf{1a}]_0/[\mathbf{2a}]_0/[t\text{-Bu-P}_4]_0$ ratio of 50/1/1. The polymerization was further continued by the subsequent addition of 50 equiv of **1b** with respect to **2a** to afford **IIa** with the $M_{n,NMR}$ of 21 900 g mol⁻¹ and M_w/M_n of 1.04 in 90% yield. The SEC trace of poly-**1a** was completely shifted to the high molecular weight region after the subsequent polymerization of **1b**, indicating the successful block copolymerization of **1a** and **1b** (Figure 1a). The ¹H NMR spectrum of **IIa** showed signals due to both the poly-**1a** and poly-**1b** along with the minor signals due to the 3-phenyl-1-propoxy group at 2.68 and 1.85 ppm, confirming that the obtained **IIa** possesses an initiator moiety at the α -chain end (Figure 2). Noteworthy is that the block copolymerization

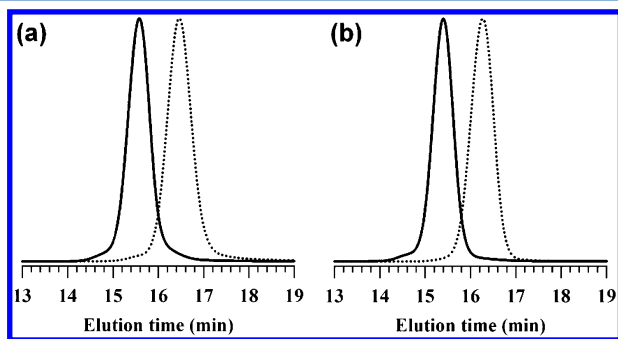


Figure 1. SEC traces of (a) **IIa** and (b) **IIb**. The dashed lines show the poly-**1a** and poly-**1b** obtained by the first polymerization.

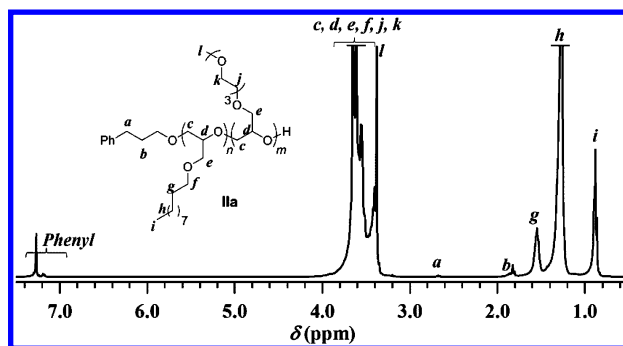


Figure 2. ¹H NMR spectrum of **IIa** in CDCl₃ (400 MHz).

of **1a** and **1b** with the opposite monomer addition sequence also produced the corresponding block copolymer, **IIb**, with the $M_{n,NMR}$ of 21 800 g mol⁻¹ and M_w/M_n of 1.05 (Figure 1b).

The intramolecular click cyclization of α -ethynyl, ω -azido end-functionalized polymers is one of the most successful methods to effectively produce cyclic polymers.^{35,36} We also demonstrated that the combination of the $t\text{-Bu-P}_4$ -catalyzed ROP and click cyclization is an effective method to produce well-defined cyclic polyethers.^{38,40} Utilizing the established procedure, the cyclic amphiphilic BCP, **III**, was synthesized through three reaction steps as shown in Scheme 3: (1) the block copolymerization of **1a** and **1b** initiated from 6-azido-1-hexanol (**2b**) to form the α -azido-functionalized poly-**1a**-block-poly-**1b** (**3a**), (2) the modification of the terminal hydroxyl group into the propargyl group to form the α -azido, ω -ethynyl-functionalized poly-**1a**-block-poly-**1b** (**3b**), and (3) the intramolecular click cyclization. The $t\text{-Bu-P}_4$ -catalyzed ROP of **1a** using 6-azido-1-hexanol (**2b**) as the initiator was performed with the $[\mathbf{1a}]_0/[\mathbf{2b}]_0/[t\text{-Bu-P}_4]_0$ ratio of 50/1/1, and the monomer conversion of **1a** reached >99% after 20 h of polymerization. The NMR and SEC measurements for the aliquot sample verified the formation of the α -azido-functionalized poly-**1a** with the number-average molecular weight ($M_{n,NMR}$) of 11 000 g mol⁻¹ and M_w/M_n value of 1.05. The subsequent addition of 50 equiv of **1b** (with respect to **2b**) to the polymerization mixture allowed the block copolymerization to produce **3a** with $M_{n,NMR}$ of 22 000 g mol⁻¹. The SEC trace of **3a** was completely shifted to the higher molecular weight region as compared to that of the poly-**1a** obtained by the first polymerization while retaining the narrow M_w/M_n of 1.05 (Figure 3a). The hydroxyl ω -chain end of **3a** was then treated with propargyl bromide in the presence of sodium hydride to produce **3b** ($M_{n,NMR} = 21 900$ g mol⁻¹, $M_w/M_n = 1.04$). The quantitative introduction of the propargyl group was verified by comparing the integration ratio of the signals due to the methylene adjacent to the azido group (proton *a* in Figure 3b) at 3.26 ppm and the methylene adjacent to the ethynyl group (proton *A*) at 4.40 ppm. The α -azido, ω -ethynyl-functionalized linear precursor, **3b**, was subjected to the intramolecular click cyclization with the CuBr/*N,N,N',N'',N''*-pentamethyldiethylenetriamine (PMDETA) catalyst system in DMF at 120 °C. To ensure highly diluted conditions, the DMF solution of **3b** (40 g L⁻¹) was slowly (0.3 mL h⁻¹) added to the catalyst solution in DMF (27.5 mL). After completing the addition, propargyl-functionalized Wang resin (PSt-C \equiv CH)⁴² was added to the reaction mixture to completely remove the unreacted **3b**, and the absence of the starting material **3b** after the reaction was confirmed by an FT-IR analysis, in which the absorption at 2100 cm⁻¹ due to the azido group completely disappeared

Scheme 3. Synthesis of Cyclic Amphiphilic Block Copolyether

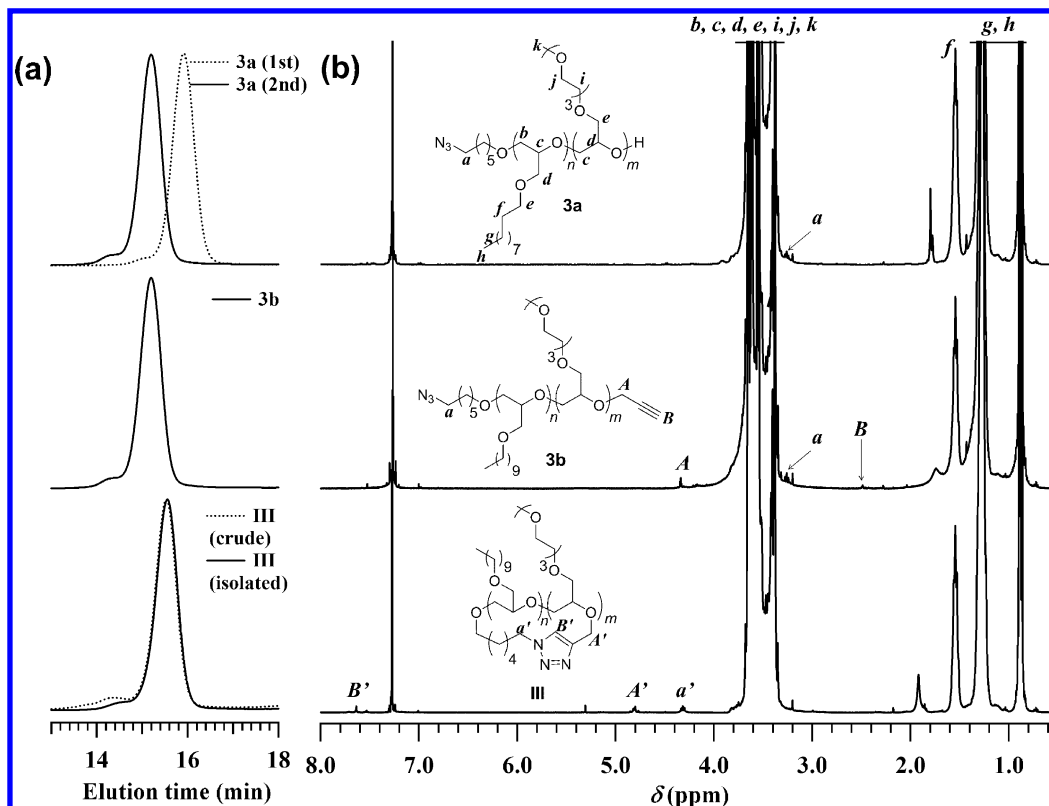
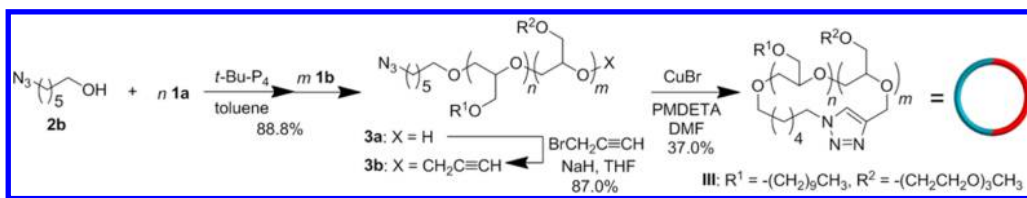


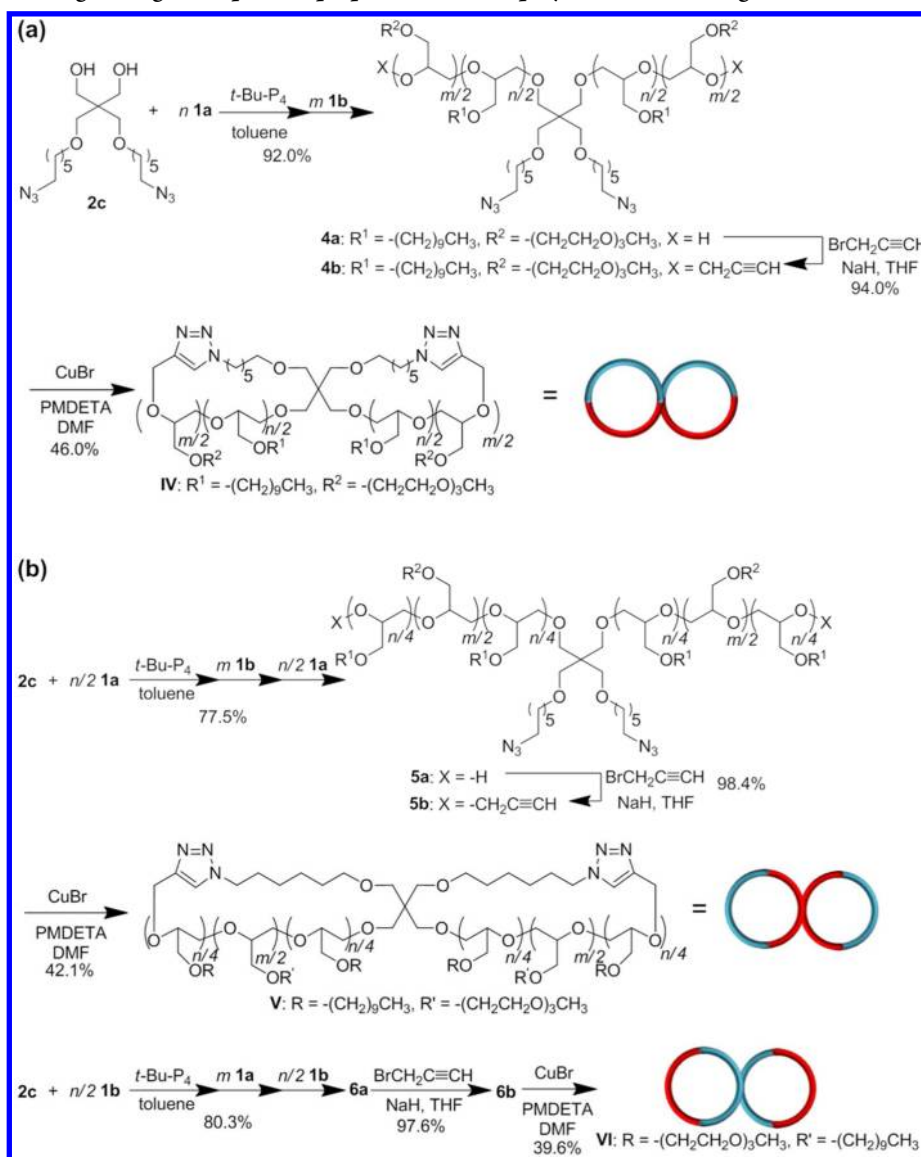
Figure 3. (a) SEC traces of **3a** (dashed line, poly-**1a** obtained by the first polymerization; solid line, **3a** obtained by the second polymerization), **3b**, and **III** (dashed line, before purification; solid line, after the purification using preparative SEC). (b) ^1H NMR spectra of **3a**, **3b**, and **III** in CDCl_3 (400 MHz).

(Figure S4). Although ca. 7% of a high molecular weight elution peak due to byproducts formed by intermolecular click reaction was observed in the SEC trace, the cyclic diblock copolymer, **III** ($M_{n,\text{NMR}} = 22\,300\text{ g mol}^{-1}$), was isolated after the purification using preparative SEC as a light brown waxy solid in 37.0% yield. The cyclized product **III** displayed a unimodal elution peak with the M_w/M_n value of 1.04 (Figure 3a). A decrease in the elution volume was observed from the starting materials **3b** to **III** (Figure 3a), indicating the formation of a cyclic product having a hydrodynamic volume smaller than the linear precursor. The ratio between the $M_{n,\text{SECs}}$ at the peak top of **III** and **3b**, i.e., $M_{n,\text{p(cyclic)}}/M_{n,\text{p(linear)}} = \langle G \rangle$, was determined to be 0.80 (Table S2), which was in good agreement with the reported value for the monocyclic poly(butylene oxide) ($\langle G \rangle = 0.69\text{--}0.81^{40}$). This is strong evidence for the intramolecular cyclization to form the cyclic polymer. Furthermore, the shrinking factor, g' , based on the intrinsic viscosities of **III** ($[\eta]_{\text{cyclic}} = 8.0\text{ mL g}^{-1}$) and **3b** ($[\eta]_{\text{linear}} = 13.1\text{ mL g}^{-1}$), i.e., $g' = [\eta]_{\text{cyclic}}/[\eta]_{\text{linear}} = 0.61$ (Table S2), also supported the decrease in the hydrodynamic volume due to cyclization. The ^1H NMR comparison of **3b** and **III** confirmed that the signals due to the methylene adjacent to the

azido group (proton *a*; 3.26 ppm), ethynyl proton (proton *B*; 2.50 ppm), and methylene adjacent to the ethynyl group (proton *A*; 4.40 ppm) of **3b** were replaced after the click reaction by a methine proton of the newly formed triazole ring (proton *B'*; 7.60 ppm) and two methylene protons adjacent to the triazole ring (protons *a'* and *A'*; 4.33 and 4.80 ppm). Thus, the desired cyclic block copolyether, **III**, was obtained by the intramolecular click cyclization of the α -azido, ω -ethynyl-functionalized linear precursor.

The intramolecular click cyclization was further applied to produce four types of figure-eight-shaped BCPs using the appropriate linear precursors with azido and ethynyl functionalities, as depicted in Schemes 4 and 5. First, a triblock copolymer bearing two azido groups at the chain center, **4a**, was prepared by the *t*-Bu- P_4 -catalyzed sequential block copolymerization of **1a** (50 equiv) and following **1b** (50 equiv) using 2,2-bis((6-azidohexyloxy)methyl)propane-1,3-diol (**2c**) as the initiator. The progress of the block copolymerization was followed by SEC measurements, and the elution peak of the polymer obtained by the first polymerization of **1a** shifted to a higher molecular weight region by the second polymerization of **1b** while retaining a narrow molecular weight

Scheme 4. Synthesis of Figure-Eight-Shaped Amphiphilic Block Copolyethers Consisting of the Same Two Cyclic Units



distribution (Figure 4a). The presence of the initiator moiety was confirmed by the signal due to the methylene proton adjacent to the azido group (proton *a* in Figure 4b). In a similar fashion, the pentablock copolymers, **5a** and **6a**, were prepared by the sequential block copolymerizations using **2c** as the initiator with the following monomer addition sequence: 25 equiv of **1a** → 50 equiv of **1b** → 25 equiv of **1a** for **5a** and 25 equiv of **1b** → 50 equiv of **1a** → 25 equiv of **1b** for **6a**. The SEC results clearly demonstrated the progress of the sequential block copolymerizations (Figure S5). For all the block copolymerizations, the full conversion of the monomer was ensured by the NMR measurement of the aliquot of the reacting mixture before adding the next monomer. The $M_{n,\text{NMR}}$ values of **4a**, **5a**, and **6a** (21 800, 22 100, and 22 000 g mol^{-1} for **4a**, **5a**, and **6a**, respectively) well agreed with the predicted value (22100 g mol^{-1}), and the M_w/M_n values were in the range of 1.04–1.08. The treatment of **4a**, **5a**, and **6a** with propargyl bromide in the presence of sodium hydride produced **4b**, **5b**, and **6b**, which was confirmed by the signals due to the ethynyl proton (proton *B* in Figure 4b) and methylene proton adjacent to the ethynyl group (proton *A*). The α,α'

diazido, ω,ω' -diethynyl linear BCP precursors **4b**, **5b**, and **6b** were then subjected to the click cyclization using the same conditions for the synthesis of **III**. The figure-eight-shaped BCPs, **IV** ($M_{n,\text{NMR}} = 21\,800 \text{ g mol}^{-1}$, $M_w/M_n = 1.06$), **V** ($M_{n,\text{NMR}} = 22\,300 \text{ g mol}^{-1}$, $M_w/M_n = 1.03$), and **VI** ($M_{n,\text{NMR}} = 22\,200 \text{ g mol}^{-1}$, $M_w/M_n = 1.03$), were obtained as a light brown waxy solid by purification using an alumina column and preparative SEC in 39.6–46.0% yields. In the SEC traces of the crude products, ca. 14%, 16%, and 21% of high molecular weight byproducts were detected for the click cyclization of **4b**, **5b**, and **6b**, respectively. The ^1H NMR analyses of the isolated figure-eight-shaped BCPs confirmed the absence of the azido and ethynyl groups as well as the formation of triazole rings (Figure 4b, Figures S6 and S7). For example, the ^1H NMR spectrum of **IV** exhibited a signal due to the triazol methine (proton *B'*) at 7.56 ppm and methylenes adjacent to the triazole ring (proton *a'* and *A'*) at 4.33 and 4.79 ppm, while the signals due to the propargyl group and methylene adjacent to the azido group disappeared (Figure 4b). The IR analysis also confirmed the absence of the azido group in the isolated products (Figure S8). Moreover, the cyclized structures for the

Scheme 5. Synthesis of Figure-Eight-Shaped Amphiphilic Block Copolyethers Consisting of Two Different Cyclic Units

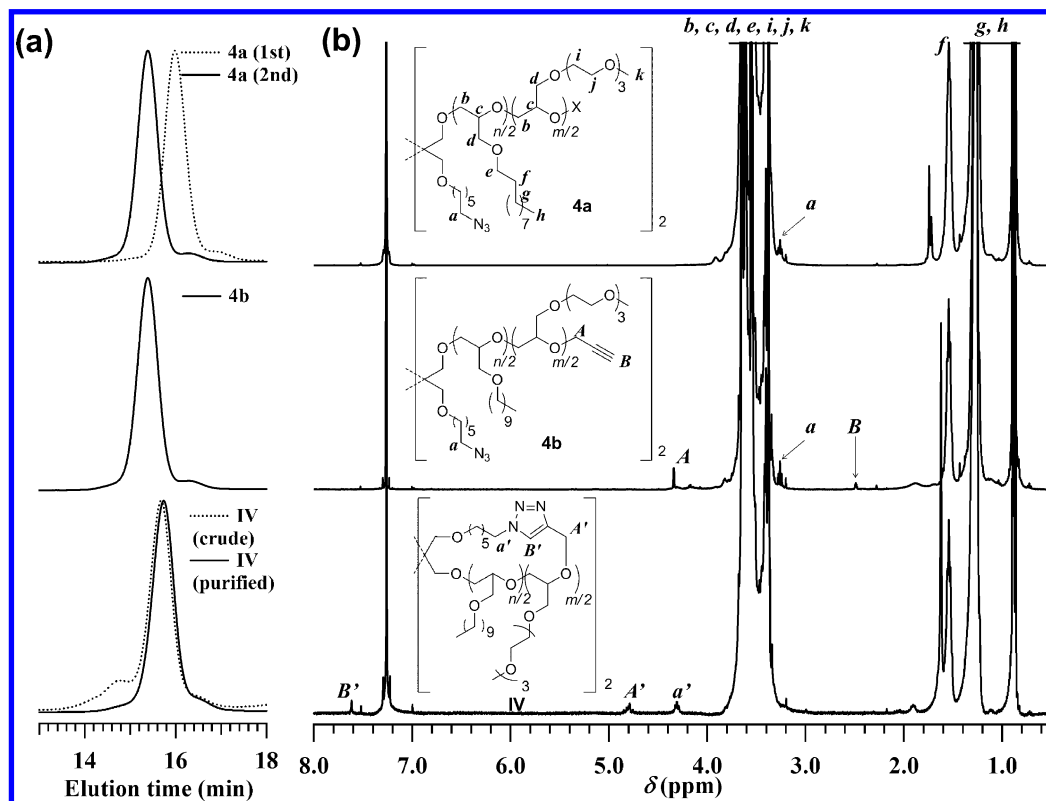
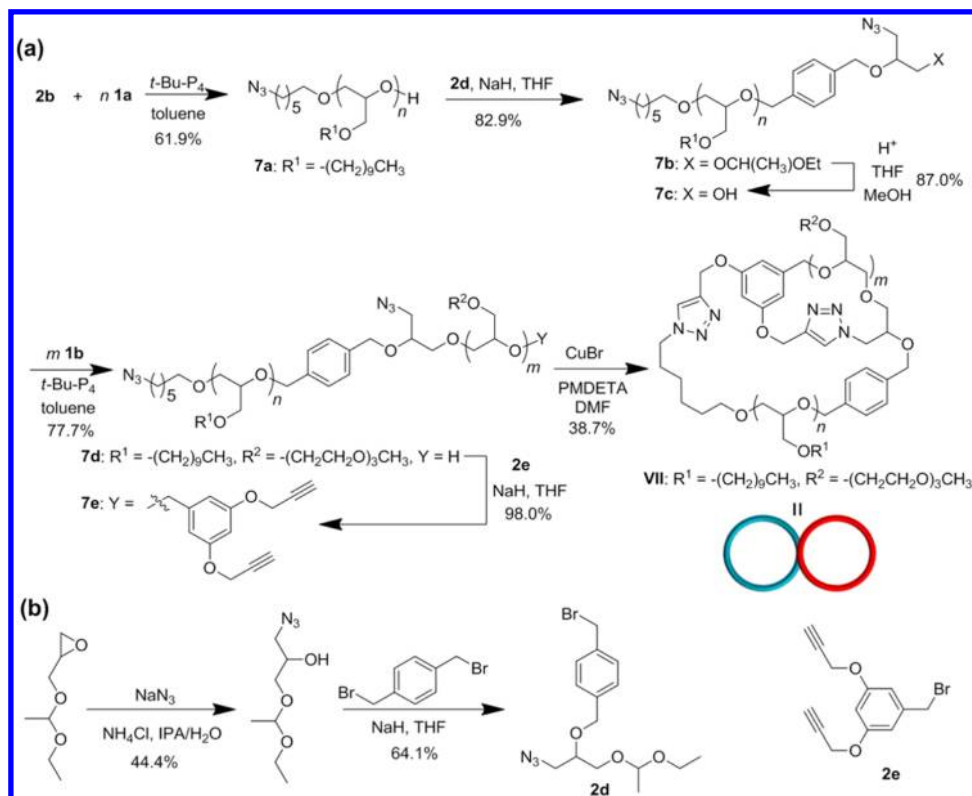


Figure 4. (a) SEC traces of $\mathbf{4a}$ (dashed line, poly- $\mathbf{1a}$ obtained by the first polymerization; solid line, $\mathbf{4a}$ obtained by the second polymerization), $\mathbf{4b}$, and $\mathbf{4c}$ (dashed line, before purification; solid line, after the purification by preparative SEC). (b) ^1H NMR spectra of $\mathbf{4a}$, $\mathbf{4b}$, and $\mathbf{4c}$ in CDCl_3 (400 MHz).

obtained BCPs were established by the longer elution time in the SEC trace as compared to the linear precursors as well as

the decrease in the intrinsic viscosity. For example, the SEC trace shifted to the lower molecular weight region after the click

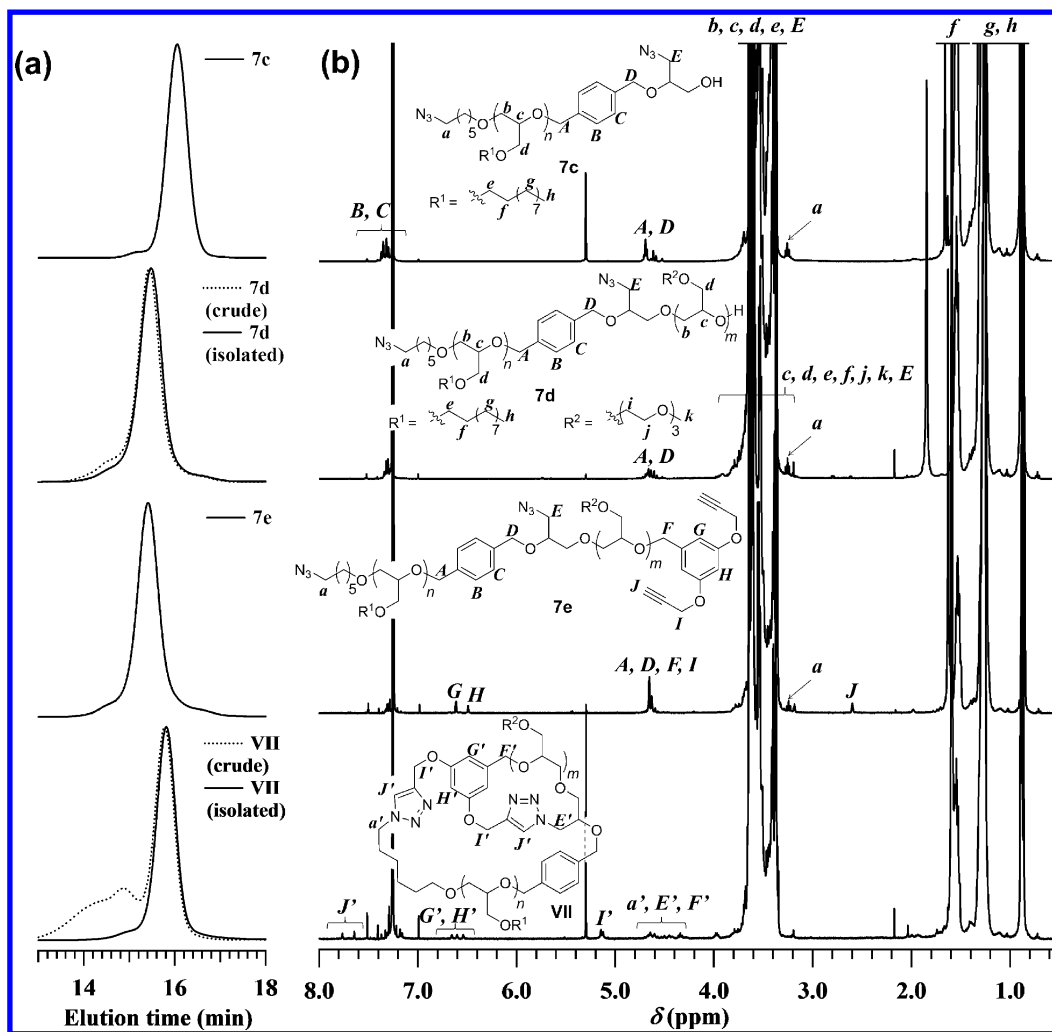


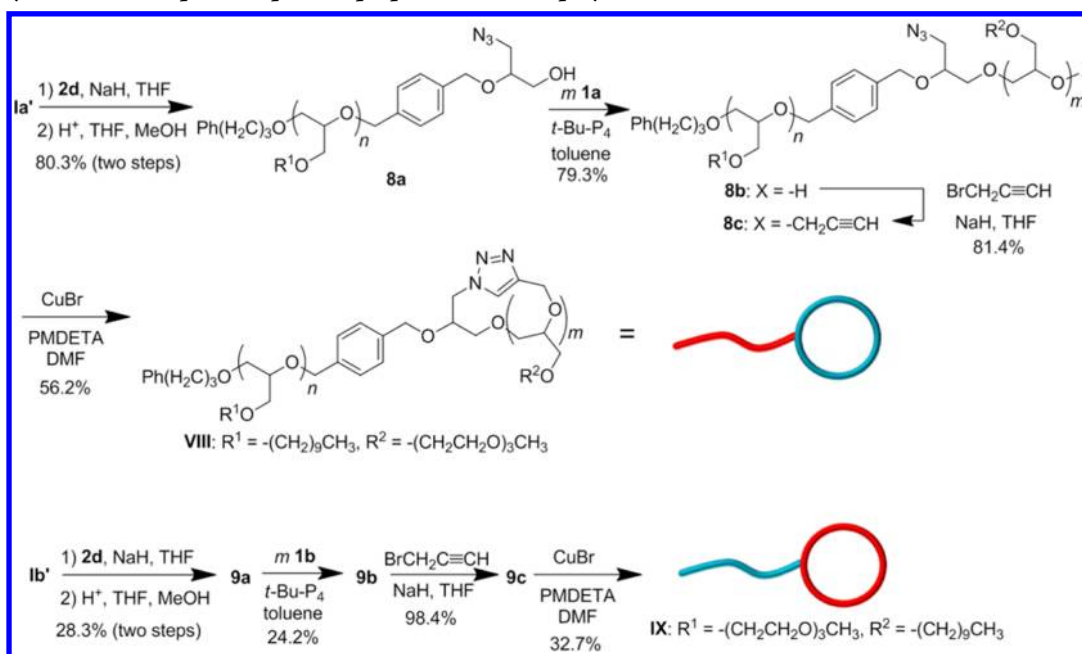
Figure 5. (a) SEC traces of **7c**, **7d** (dashed line, before purification; solid line, after the purification using preparative SEC), **7e**, and **VII** (dashed line, before purification; solid line, after the purification using preparative SEC). (b) ^1H NMR spectra of **7c**, **7d**, **7e**, and **VII** in CDCl_3 (400 MHz).

reaction of **4b** to form **IV** (Figure 4a), and the $\langle G \rangle$ value was calculated to be 0.80 (Table S3), which was in good agreement with that of the figure-eight-shaped poly(butylene oxide) ($\langle G \rangle = 0.65\text{--}0.83^{40}$). The g' values of **IV**, **V**, and **VI** were in the range of 0.46–0.56 (Table S3) and were lower than that of **III**, indicating the more compact conformations of **IV**, **V**, and **VI** than the monocyclic **III**. Thus, the three types of figure-eight-shaped BCPs with different distributions of hydrophilic and hydrophobic blocks were obtained by the double click cyclization of the multiblock type precursors having two ethynyl groups at the ω -chain ends and two azido groups at the chain center.

The next target is the figure-eight-shaped BCP consisting of two different cyclic units, **VII**, which is in contrast to the above-prepared figure-eight-shaped BCPs having the same two cyclic units. Our synthetic strategy for **VII** is based on the double click cyclization of a linear diblock copolymer of **1a** and **1b** bearing two ethynyl groups at the ω -chain end and two azido groups at the α -chain end and the chain center (**7e**), as shown in Scheme 5a. To synthesize the diblock copolymer having two azido groups at the α -chain end and the chain center (**7d**), we first prepared the α,ω -diazido, ω -hydroxyl poly-**1a** (**7b**), in which the hydroxyl group would be used as the initiation site for the subsequent chain extension. We newly designed and synthesized 1-(((1-azido-3-(1-ethoxyethoxy)propan-2-yl)oxy)-

methyl)-4-(bromomethyl)benzene (**2d**) as the terminator for introducing both the azido and hydroxyl groups at the ω -chain end. **2d** was prepared by the ring-opening of ethoxyethyl glycidyl ether using sodium azide in the presence of ammonium chloride followed by the treatment with an excess amount of α,α -dibromo-*p*-xylene, as shown in Scheme 5b. An α -azido end-functionalized poly-**1a** (**7a**, $M_{n,\text{NMR}} = 10\,900$, $M_w/M_n = 1.02$) was treated with **2d** in the presence of sodium hydride, and the ethoxyethyl group was then deprotected under acidic conditions to give **7c**. The ^1H NMR spectrum of **7c** showed the signals due to the benzyl protons (protons **A** and **D** in Figure 5b) at 4.70 ppm as well as methylene protons adjacent to the azido group (protons **a**) at 3.26 ppm, from which the quantitative introduction of an azido and a hydroxyl group at the ω -chain end was verified. After a rigorous dehydration, **7c** was utilized as a macroinitiator for the synthesis of a diblock copolymer of **1a** and **1b** with two azido groups at the α -chain end and the junction point of the two blocks, **7d**. The polymerization was carried out at the $[\mathbf{1b}]_0/[\mathbf{7c}]_0/[\textit{t}\text{-Bu-P}_4]_0$ ratio of 50/1/1 to give **7d** in 77.7% yield. The SEC trace of **7c** shifted to the higher molecular weight region after the polymerization (Figure 5a), which confirmed that the polymerization was initiated from the hydroxyl group of **7c**. The $M_{n,\text{NMR}}$ and M_w/M_n of the isolated **7d** were determined to be 22 000 g mol^{-1} and 1.06, respectively. **7d** was then further converted to

Scheme 6. Synthesis of Tadpole-Shaped Amphiphilic Block Copolyethers



the requisite linear precursor, **7e** ($M_{n,NMR} = 22\,100\text{ g mol}^{-1}$, $M_w/M_n = 1.05$), by the treatment with 1-bromomethyl-3,5-bis(2-propynyloxy)benzene (**2e**) in the presence of sodium hydride. The double click cyclization of **7e** and SEC fractionation led to the desired **VII** with the $M_{n,NMR}$ and M_w/M_n of $22\,200\text{ g mol}^{-1}$ and 1.04, respectively, in 38.7% yield. Here, ca. 38% of high molecular weight byproducts formed through the intermolecular click reaction were detected in the SEC trace of the crude product. The ^1H NMR and IR spectroscopic analyses proved that there were no unreacted azido and ethynyl groups (Figure 5b and Figure S8), implying that the obtained product should have a doubly cyclized structure. In addition, the ^1H NMR spectrum of **VII** showed two signals due to the triazole methine protons (proton *J'* in Figure 5b) at 7.76 and 7.64 ppm. The increase in the SEC elution volume (Figure 5a; $\langle G \rangle = 0.75$) as well as decrease in the intrinsic viscosity ($g' = 0.60$) also provided evidence of the doubly cyclized architecture of the product. Therefore, the synthesis of a series of figure-eight-shaped amphiphilic BCPs with four different types of hydrophobic/hydrophilic orientations has been achieved via the double click cyclization of diazido,diethynyl-functionalized linear precursors.

The synthesis of the tadpole-shaped BCPs were attempted as illustrated in Scheme 6. Poly-**1a** having a 3-phenyl-1-propoxy α -chain end (**1a'**, $M_{n,NMR} = 11\,100\text{ g mol}^{-1}$, $M_w/M_n = 1.05$) was modified by the treatment with **2d** and following deprotection of the ethoxyethyl group, providing ω -azido, ω -hydroxyl-functionalized poly-**1a**, **8a**. The *t*-Bu- P_4 -catalyzed ROP of **1b** using **8a** as a macroinitiator followed by treatment with propargyl bromide led to the poly-**1a**-block-poly-**1b** with an ethynyl group at the ω -chain end and an azido group at the junction point between the two blocks, **8c** ($M_{n,NMR} = 22\,400\text{ g mol}^{-1}$, $M_w/M_n = 1.05$). An analogue of **8c** with the opposite block sequence, **9c** ($M_{n,NMR} = 22\,100\text{ g mol}^{-1}$, $M_w/M_n = 1.05$), was prepared in a similar fashion, beginning with poly-**1b** having the 3-phenyl-1-propoxy α -chain end (**1b'**, $M_{n,NMR} = 10\,900\text{ g mol}^{-1}$, $M_w/M_n = 1.06$). The click cyclization of **8c** and following SEC fractionation gave the desired tadpole-shaped

BCPs consisting of a hydrophilic cyclic unit and a hydrophobic tail, **VIII** ($M_{n,NMR} = 21\,900\text{ g mol}^{-1}$, $M_w/M_n = 1.04$), in 56.2% yield. In a similar fashion, the tadpole-shaped BCPs consisted of a hydrophobic cyclic unit and a hydrophilic tail, **IX** ($M_{n,NMR} = 22\,400\text{ g mol}^{-1}$, $M_w/M_n = 1.06$), was obtained in 32.7% yield. Although 23% and 20% of byproducts were formed during the cyclization reaction of **8c** and **9c**, respectively, as indicated by the SEC traces of the crude products, these were removed through the SEC fractionation process. The chemical structures of **VIII** and **IX** were confirmed by IR and NMR analyses, in which the disappearances of the azido and ethynyl groups as well as the formation of the triazole ring were observed (Figures S9–S11). The cyclized architectures for **VIII** and **IX** were further verified by the $\langle G \rangle$ values (0.88 for **VIII** and 0.91 for **IX**; Figure S12 and Table S4) as well as the g' values (0.88 for **VIII** and 0.68 for **IX**, Table S4).

For the preliminary study on regarding effect of the cyclic architecture, we investigated the self-assembly of the linear (**IIa**), cyclic (**III**), figure-eight-shaped (**IV**, **V**, **VI**, and **VII**), and

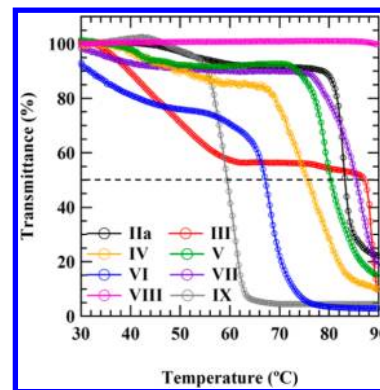


Figure 6. Temperature dependence of optical transmittance at 300 nm obtained for 0.50 g L^{-1} aqueous solution of linear (**IIa**), cyclic (**III**), figure-eight-shaped (**IV**, **V**, **VI**, and **VII**), and tadpole-shaped BCPs (**VIII** and **IX**).

Table 1. Molecular Characteristic, Critical Micelle Concentration (CMC), Hydrodynamic Diameter ($2R_h$), and Cloud Point (T_c) of Linear (IIa), Cyclic (III), Figure-Eight-Shaped (IV, V, VI, and VII), and Tadpole-Shaped BCPs (VIII and IX)

sample	architecture	$M_{n,NMR}^a$ (g mol ⁻¹)	M_w/M_n^b	DP _a /DP _b ^c	CMC ^d (mg L ⁻¹)	$2R_h^e$ (nm)	T_c^f (°C)
IIa	linear	21 900	1.04	50/51	1.4	123	83
III	cyclic	22 300	1.04	51/50	1.8	166	87
IV	figure-eight shape	21 800	1.06	50/48	1.5	138	75
V		22 300	1.03	52/48	1.0	179	80
VI		22 200	1.03	50/50	1.4	171	67
VII		22 200	1.04	50/50	1.2	221	85
VIII	tadpole shape	21 900	1.04	51/49	1.4	83	n.d. ^g
IX		22 400	1.06	51/50	3.4	170	59

^aDetermined by ¹H NMR. ^bDetermined by SEC in THF. ^cNumber-average degree of polymerizations of decyl glycidyl ether (DP_a) and triethylene glycol methyl glycidyl ether (DP_b) in the copolymer were determined by ¹H NMR. ^dDetermined by steady-state fluorescence method using pyrene as a probe at 25 °C. ^eDetermined based on multiangle DLS measurements (concentration, 0.50 g L⁻¹; temperature, 25 °C). ^fDetermined by turbidimetric analysis (concentration, 0.50 g L⁻¹). T_c was defined by the temperature at which the transmittance of sample solution reached 50%. ^g T_c was not observed upon the heating up to 90 °C.

tadpole-shaped (VIII and IX) amphiphilic BCPs in water. The micelle solutions (concentration 0.50 g L⁻¹) were prepared by the direct dissolution of the BCPs in pure water at room temperature by sonication. The dynamic light scattering (DLS) experiment was employed to investigate the size of the aggregates (Figure S13). The intensity-average size distribution of every BCP aqueous solution displayed a monomodal peak corresponding to the aggregates formed through the self-assembling process. Multiangle DLS measurements for the solutions revealed the linear dependence of the relaxation frequency ($\Gamma = 1/\tau$) on the square of the wavevector (q^2), which clearly indicated the Brownian diffusive motion (see Supporting Information). The slope is equal to the diffusion coefficient (D) of the aggregates in water, from which the hydrodynamic diameter ($2R_h$) was calculated by the Stokes–Einstein relation and was in the range of 83–221 nm (Table 1). The R_h values of the BCPs were apparently greater than those of the fully extended chain lengths (approximately 36 nm for linear BCP, 18 nm for cyclic and figure-eight-shaped BCPs, 27 nm for tadpole-shaped BCPs, in which the DP and molecular length of a monomer unit were assumed to be 100 and 0.358 nm,⁴³ respectively), suggesting that the aggregates of every BCP were large compound micelles or vesicles. The actual morphologies of the aggregates were then confirmed by transmission electron microscopy (TEM), in which all of the samples were observed without staining. The TEM images revealed the presence of hard-sphere-like nanoparticles or its agglomerates in all case (Figure S14), leading to the conclusion that all of the aggregates consisted of large compound micelles. Therefore, the cyclic architecture of the BCP as well as the block arrangement would have a small impact on the morphology of the aggregate in water. The critical micelle concentrations (CMC) for the BCPs in water were determined by a fluorescence technique using pyrene as the fluorescence probe at 25 °C (Figure S15). There is no distinctive difference in the CMC values among the BCPs (1.0–3.4 mg L⁻¹, Table 1), indicating that the CMC value is not significantly affected by the cyclic topology as well as the block arrangement. Booth et al. reported that the CMCs of cyclic poly(ethylene oxide)-*block*-poly(propylene oxide) and its linear precursor were very similar.³⁴ The cloud point (T_c) for the aggregates, a measure of their thermal stability,⁴² were determined by the variable-temperature UV–vis absorption measurements of the aqueous BCP solutions. The transmittance at 300 nm was monitored during the continuous heating at the 1.0 °C min⁻¹ heating ratio,

and T_c was defined as the temperature at which the transmittance of the sample solution reached 50%. Every BCP, except for VIII, exhibited the characteristic phase transition phenomenon at the T_c ranging from 59 to 87 °C, whereas VIII exhibited no such phase transition up to 90 °C. Although the difference in the polymer structures among the BCPs is only the macromolecular architecture, a significant variation in T_c was observed, which should provide an interesting insight into the thermal stabilities of the aggregates depending on the cyclic architecture. The cyclic amphiphilic BCP III showed a T_c at 87 °C, which was 4 °C higher than that of the linear counterpart IIa ($T_c = 83$ °C). The increased T_c value of III with respect to IIa should be ascribed to the restricted intermicelle linking due to the looped conformation of the hydrophilic block at the shell region. In contrast, the figure-eight-shaped BCP IV, which can be regarded as a dimeric analogue of III, showed a lower T_c value of 75 °C. A significant difference in the T_c was observed between VIII ($T_c > 90$ °C) and IX ($T_c = 59$ °C), though both of them were categorized as having a tadpole-shaped architecture. Given that the aggregate of VIII and IX is surrounded by the shell of hydrophilic cyclic and linear poly-1b, respectively, these results suggest that the cyclic architecture of the shell-forming block contributes to the increase in the T_c by reducing the intermicelle linking as a consequence of their restricted chain mobility and lower entanglement nature. These results also implied that the cyclic architecture of the core-forming block led to a decrease in the T_c with respect to the corresponding linear diblock counterpart. The similar T_c values among the figure-eight-shaped BCPs consisting of discrete hydrophobic and hydrophilic cyclic units, VII and IIa, are understandable due to the balancing out of two such effects. On the other hand, the lower T_c values for the figure-eight-shaped BCPs, IV, V, and VI, with respect to IIa could not be explained by such effects due to their complicated chain packing at the interface of the micelle core and shell. Given that V and VI are regarded as the analogue of the poly-1b-*block*-poly-1a-*block*-poly-1b and poly-1a-*block*-poly-1b-*block*-poly-1a triblock copolymers, respectively, an interesting comparison can be made between their T_c values. The relatively low T_c values of the triblock copolymers with hydrophobic end blocks with respect to those of the opposite block arrangement were reported for the poly(ethylene oxide)/poly(propylene oxide) and poly(ethylene oxide)/poly(butylene oxide) triblock copolymer systems. This effect is related to the intermicelle linking through the hydrophobic end blocks.³²

Therefore, the lower T_c value of VI than that of V should be ascribed to the enhanced intermicelle linking due to the hydrophobic end block.

CONCLUSION

We have demonstrated the synthesis of systematic sets of figure-eight- and tadpole-shaped amphiphilic BCPs together with the corresponding linear and cyclic BCP counterparts via the *t*-Bu-P₄-catalyzed ROP of hydrophobic and hydrophilic glycidyl ethers. The well-controlled nature of the ROP system allowed us to attain a series of azido- and ethynyl-functionalized di-, tri-, and multiblock copolymers with a predicted molecular weight, monomer composition, and narrow molecular weight distribution, which led to produce the corresponding cyclic-containing amphiphilic BCPs via the intramolecular click cyclization. Our preliminary studies on the self-assembly of the linear, cyclic, figure-eight-shaped, and tadpole-shaped amphiphilic BCPs in water revealed the significant variation in the T_c values depending on the cyclic topology, though there were small topological effects on their CMC value and morphology of the aggregates. However, further detailed investigations should be necessary to fully understand the aqueous self-assembling properties associated with the cyclic architectures. Considering the functional group loading capacity of the glycidyl ether-based BCPs, the present synthetic strategy provides a wide array of BCP systems with cyclic-containing architectures, which would be used as a model system for investigating the topological effect of the BCP self-assembly in both the solution and bulk states. On the basis of this versatile synthetic strategy, we are currently trying to investigate the topological effects on the microphase separation leading to various nanostructures.

ASSOCIATED CONTENT

Supporting Information

Experimental section and additional data (¹H NMR, MALDI-TOF MS, IR, SEC, DLS, TEM, and CAC data). This material is available free of charge via the Internet at <http://pubs.acs.org>.

AUTHOR INFORMATION

Corresponding Authors

*E-mail satoh@poly-bm.eng.hokudai.ac.jp (T.S.).

*E-mail kakuchi@poly-bm.eng.hokudai.ac.jp (T.K.).

Notes

The authors declare no competing financial interest.

ACKNOWLEDGMENTS

This work was financially supported by the MEXT program "Strategic Molecular and Materials Chemistry through Innovative Coupling Reactions" of Hokkaido University, the MEXT Grant-in-Aid for Challenging Exploratory Research (Grant 25620089), and the MEXT Grant-in-Aid for Scientific Research on Innovative Areas "Advanced Molecular Transformation by Organocatalysts". T.I. was funded by the JSPS Fellowship for Young Scientists.

REFERENCES

- (1) Hadjichristidis, N.; Pitsikalis, M.; Pispas, S.; Iatrou, H. *Chem. Rev.* **2001**, *101*, 3747–3792.
- (2) Hadjichristidis, N.; Iatrou, H.; Pitsikalis, M.; Mays, J. *Prog. Polym. Sci.* **2006**, *31*, 1068–1132.
- (3) Yamamoto, T.; Tezuka, Y. *Polym. Chem.* **2011**, *2*, 1930–1941.

- (4) Laurent, B. A.; Grayson, S. M. *Chem. Soc. Rev.* **2009**, *38*, 2202–2213.
- (5) Jia, Z.; Monteiro, M. J. *J. Polym. Chem., Part A: Polym. Chem.* **2012**, *50*, 2085–2097.
- (6) Kricheldorf, H. R. *J. Polym. Chem., Part A: Polym. Chem.* **2010**, *48*, 251–284.
- (7) Honda, S.; Yamamoto, T.; Tezuka, Y. *J. Am. Chem. Soc.* **2010**, *132*, 10251–10253.
- (8) Honda, S.; Yamamoto, T.; Tezuka, Y. *Nat. Commun.* **2013**, *4*, 1574.
- (9) Heo, K.; Kim, Y. Y.; Kitazawa, Y.; Kim, M.; Jin, K. S.; Yamamoto, T.; Ree, M. *ACS Macro Lett.* **2014**, *3*, 233–239.
- (10) Zhu, Y.; Gido, S. P.; Iatrou, H.; Hadjichristidis, N.; Mays, J. W. *Macromolecules* **2003**, *36*, 148–152.
- (11) Takano, A.; Kadoi, O.; Hirahara, K.; Kawahara, S.; Isono, Y.; Suzuki, J.; Matsushita, Y. *Macromolecules* **2003**, *36*, 3045–3050.
- (12) Poelma, J. E.; Ono, K.; Miyama, D.; Aida, T.; Satoh, K.; Hawker, C. J. *ACS Nano* **2012**, *6*, 10845–10854.
- (13) Iatrou, H.; Hadjichristidis, N.; Meier, G.; Frielinghaus, H.; Monkenbusch, M. *Macromolecules* **2002**, *35*, 5426–5437.
- (14) Borsali, R.; Minatti, E.; Putaux, J.-L.; Schappacher, M.; Deffieux, A.; Viville, P.; Lazzaroni, R.; Narayanan, T. *Langmuir* **2003**, *19*, 6–9.
- (15) Minatti, E.; Viville, P.; Borsali, R.; Schappacher, M.; Deffieux, A.; Lazzaroni, R. *Macromolecules* **2003**, *36*, 4125–4133.
- (16) Beinath, S.; Schappacher, M.; Deffieux, A. *Macromolecules* **1996**, *29*, 6737–6743.
- (17) Dong, Y.-Q.; Tong, Y.-Y.; Dong, B.-T.; Di, F.-S.; Li, Z.-C. *Macromolecules* **2009**, *42*, 2940–2948.
- (18) Wang, G.; Hu, B.; Fan, X.; Zhang, Y.; Huang, J. *J. Polym. Chem., Part A: Polym. Chem.* **2012**, *50*, 2227–2235.
- (19) Wang, X.; Liu, T.; Liu, S. *Biomacromolecules* **2011**, *12*, 1146–1154.
- (20) Shi, G.-Y.; Sun, J.-T.; Pan, C.-Y. *Macromol. Chem. Phys.* **2011**, *212*, 1305–1315.
- (21) Hatakeyama, F.; Yamamoto, T.; Tezuka, Y. *ACS Macro Lett.* **2013**, *2*, 427–431.
- (22) Fan, X.; Huang, B.; Wang, G.; Huang, J. *Macromolecules* **2012**, *45*, 3779–3786.
- (23) Lonsdale, D. E.; Monteiro, M. J. *J. Polym. Chem., Part A: Polym. Chem.* **2011**, *49*, 4603–4612.
- (24) Mark, H. F.; Bikales, N. M.; Overberger, C. G.; Menges, G.; Kroschwitz, J. I., Eds.; *Encyclopedia of Polymer Science and Engineering*; John Wiley & Sons, Inc.: New York, 1985; Vol. 6.
- (25) Schmolka, I. R. *J. Am. Oil Chem. Soc.* **1977**, *54*, 110–116.
- (26) Gupta, S.; Tyagi, R.; Parmar, V. S.; Sharma, S. K.; Haag, R. *Polymer* **2012**, *53*, 3053–3078.
- (27) Booth, C.; Attwood, D. *Macromol. Rapid Commun.* **2000**, *21*, 501–527.
- (28) Brocas, A.-L.; Gervais, M.; Carlotti, S.; Pispas, S. *Polym. Chem.* **2012**, *3*, 2148–2155.
- (29) Mai, S.-M.; Fairclough, J. P. A.; Terrill, N. J.; Turner, S. C.; Hamley, I. W.; Matsen, M. W.; Ryan, A. J.; Booth, C. *Macromolecules* **1998**, *31*, 8110–8116.
- (30) Halacheva, S.; Rangelov, S.; Tsvetanov, C. *Macromolecules* **2006**, *39*, 6845–6852.
- (31) Yu, G.-E.; Yang, Y.-W.; Yang, Z.; Attwood, D.; Booth, C. *Langmuir* **1996**, *12*, 3404–3412.
- (32) Altinok, H.; Yu, G.-E.; Nixon, S. K.; Gorry, P. A.; Attwood, D.; Booth, C. *Langmuir* **1997**, *13*, 5837–5848.
- (33) Yu, G.-E.; Yang, Z.; Attwood, D.; Price, C.; Booth, C. *Macromolecules* **1996**, *29*, 8479–8486.
- (34) Yu, G.-E.; Garrett, C. A.; Mai, S.-M.; Altinok, H.; Attwood, D.; Price, C.; Booth, C. *Langmuir* **1998**, *14*, 2278–2285.
- (35) Laurent, B. A.; Grayson, S. M. *J. Am. Chem. Soc.* **2006**, *128*, 4238–4239.
- (36) Lansdale, D. E.; Bell, C. A.; Monteiro, M. J. *Macromolecules* **2010**, *43*, 3331–3339.
- (37) Misaka, H.; Sakai, R.; Satoh, T.; Kakuchi, T. *Macromolecules* **2011**, *44*, 9099–9107.

- (38) Misaka, H.; Tamura, E.; Makiguchi, K.; Kamoshida, K.; Sakai, R.; Satoh, T.; Kakuchi, T. *J. Polym. Sci., Part A: Polym. Chem.* **2012**, *50*, 1941–1952.
- (39) Kwon, W.; Roh, Y.; Kamoshida, K.; Kwon, K. H.; Jeong, Y. C.; Kim, J.; Misaka, H.; Shin, T. J.; Kim, J.; Kim, K.-W.; Jin, K. S.; Chang, T.; Kim, H.; Satoh, T.; Kakuchi, T.; Ree, M. *Adv. Funct. Mater.* **2012**, *22*, 5194–5208.
- (40) Isono, T.; Kamoshida, K.; Satoh, Y.; Takaoka, T.; Sato, S.-i.; Satoh, T.; Kakuchi, T. *Macromolecules* **2013**, *46*, 3841–3849.
- (41) Hans, M.; Keul, H.; Moeller, M. *Polymer* **2009**, *50*, 1103–1108.
- (42) Rao, J.; Zhang, Y.; Zhang, J.; Liu, S. *Biomacromolecules* **2008**, *9*, 2586–2593.
- (43) Rixman, M. A.; Dean, D.; Ortiz, C. *Langmuir* **2003**, *19*, 9357–9372.